Optics Letters

Single-shot color-multiplexed quantitative phase imaging with Kramers–Kronig relations

Qian Shen,[1,2,3] Shun Zhou,[1,2,3] Kaiyu Du,[1,2,3] Yefeng Shu,[1,2,3] Habib Ullah,[1,2,3] Wenzhuo Xie,[1,2,3] Tingxiang Xiong,[1,2,3] Zhuoshi Li,[1,2,3] Zanyang Guan,[4] Yulong Li,[4] Ran Ye,[1,5] Yao Fan,[1,2,3] Qian Chen,[3,6] Jiasong Sun,[1,2,3,7] and Chao Zuo[1,2,3,*]

[1]Smart Computational Imaging Laboratory (SCILab), School of Electronic and Optical Engineering, Nanjing University of Science and Technology, Nanjing, Jiangsu Province 210094, China
[2]Smart Computational Imaging Research Institute of Nanjing University of Science and Technology, Nanjing, Jiangsu Province 210019, China
[3]Jiangsu Key Laboratory of Visual Sensing & Intelligent Perception, Nanjing, Jiangsu Province 210094, China
[4]Laser Fusion Research Center, China Academy of Engineering Physics, Mianyang 621900, China
[5]School of Computer and Electronic Information, Nanjing Normal University, Nanjing 210023, China
[6]State Key Laboratory of Extreme Environment Optoelectronic Dynamic Measurement Technology and Instrument, Taiyuan, Shanxi Province 030051, China
[7]sunjiasong@njust.edu.cn
*zuochao@njust.edu.cn

Received 3 March 2026; revised 20 April 2026; accepted 7 May 2026; posted 27 May 2026; published 26 June 2026

Single-shot quantitative phase imaging (QPI) promises high-speed, label-free observation of dynamic biological processes, but remains challenged by limited reconstruction fidelity, weak-object assumptions, and the inability to recover both amplitude and large phase delays. In this Letter, we introduce CMKK-QPI, a single-shot QPI framework that synergizes color-multiplexed oblique illumination with iterative processing based on the Kramers–Kronig (KK) relations. By spectrally encoding angular diversity into a single color exposure, CMKK-QPI enables simultaneous acquisition of multiple intensity measurements without sacrificing temporal resolution. An initial complex-field estimate is retrieved via the KK relations and iteratively refined to jointly reconstruct amplitude and phase. Experiments on resolution targets, biological tissues, and live cells demonstrate that CMKK-QPI achieves a resolution corresponding to twice the coherent diffraction limit and phase accuracy comparable to multi-frame Fourier ptychographic microscopy, with only a single exposure and convergence within 5 iterations. Importantly, CMKK-QPI robustly handles large phase variations and enables long-term, high-speed imaging of dynamic cellular morphology at 30 Hz. With minimal data redundancy and high computational efficiency, CMKK-QPI provides a practical solution for high-speed, label-free imaging of dynamic biological samples.

https://doi.org/10.1364/OL.596621

Quantitative phase imaging (QPI) has emerged as a powerful tool for label-free visualization of optically transparent specimens, enabling non-invasive characterization of cellular morphology and dynamics [1–4]. Traditional holographic QPI techniques [5,6], which rely on interferometric setups with coherent illumination, inherently suffer from stability constraints and speckle noise, limiting their practicality for dynamic biological imaging. To circumvent these challenges, non-interferometric phase retrieval methods have garnered considerable attention. Techniques such as differential phase contrast (DPC) [7,8], transport of intensity equation (TIE) [9,10], and Fourier ptychographic microscopy (FPM) [11–13] bypass the need for coherent sources and retrieve phase information directly from intensity-only measurements, offering enhanced resolution and environmental robustness.

Combined with synthetic aperture techniques, QPI can overcome the spatial bandwidth product (SBP) limit of a conventional microscope, but such methods typically require iterative reconstruction with substantial data redundancy. As a result, many raw images must be acquired, sacrificing temporal resolution and limiting their applicability to high-speed imaging. Existing single-shot synthetic-aperture QPI techniques, such as single-shot FPM (SFPM) [14], can retrieve phase from a single color image but generally assume a pure-phase object, precluding recovery of the full complex amplitude. Spectrally multiplexed imaging has also been demonstrated using color multiplexing and space-domain Kramers–Kronig (KK) relations [15,16], but this approach does not enable iterative recovery of absorption and large phase delays. In addition, non-interferometric QPI techniques usually rely on approximation conditions such as the first-order Born approximation (weak-object approximation) [17], making it difficult to reconstruct objects with a high phase dynamic range. For brevity, we refer to such specimens as large-phase objects below. These limitations motivate the development of a single-shot QPI framework capable of recovering both absorption and large phase variations.

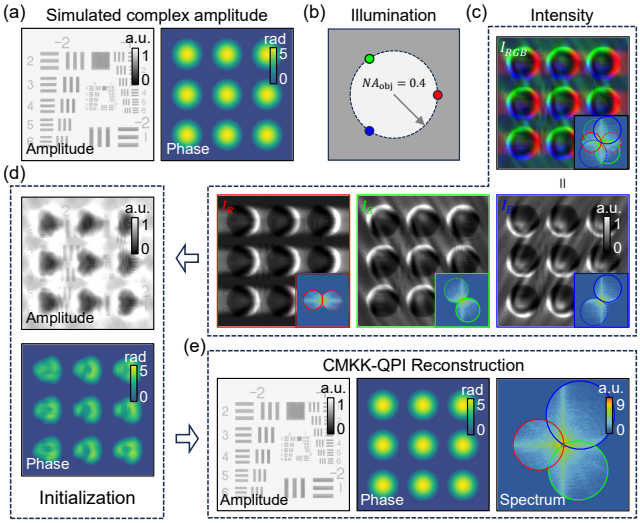

Fig. 1. Flowchart of CMKK-QPI. (a) Simulated complex amplitude. (b) Color-multiplexed illumination pattern. (c) Captured raw image and its decomposition into the R, G, and B channels. (d) KK initialization. (e) CMKK-QPI reconstruction.

In this Letter, based on the iKK-QPI framework [18], we introduce a color-multiplexed scheme termed CMKK-QPI for single-shot reconstruction of both amplitude and phase. The method assumes negligible chromatic dispersion within the visible range, so that for weakly absorbing samples such as live cells and unstained tissue sections, the amplitude distribution is nearly identical across the red, green, and blue channels. Three intensity measurements corresponding to different incident angles are encoded simultaneously into the RGB channels of a color image sensor. The complex field for each angle is first retrieved via the KK relations [19,20], and these fields are then synthesized into an initial estimate that is further refined by iterative optimization to recover the sample amplitude and phase distributions accurately.

We implemented CMKK-QPI on the FPM platform with annular illuminations [21]. The system employs three LEDs from a programmable LED array (4 mm pitch; central wavelengths 632/525/465 nm) corresponding to R/G/B channels. By adjusting the array height, each LED element is accurately positioned at the edge of the objective's numerical aperture (NA) in the frequency domain to ensure the validity of the KK relations. This setup generates color-coded triangle oblique illumination matched to a 10×, 0.4 NA objective lens (UPlanSApo, Olympus) [Fig. 1(b)]. Raw data is acquired by a color camera (DFK 37AUX226, 1.85 μm pixel size, 30 Hz) and separated into three monochrome intensity images via a color-leakage correction algorithm [22]. In this configuration, the complex field can be reconstructed individually from each captured color frame via KK relations. Serving as an initialization, this estimate is further refined through an iterative process to reconstruct the complete amplitude and phase information. Since the full complex field is reconstructed from a single exposure, the system's imaging speed is determined by the camera's acquisition rate, thereby achieving a high frame rate of 30 Hz for dynamic monitoring.

Illustrated by the simulation of a complex amplitude sample in Fig. 1(a), the principle of CMKK-QPI is presented in Fig. 1. We implemented an annular matched illumination scheme [21,23,24], designed to optimize the information transfer of the imaging system. By positioning the unscattered light at the edge of the pupil in the Fourier plane, this setup simultaneously enables the efficient low-frequency transfer and extension of the resolution limit. Furthermore, this configuration ensures the analytic condition imposed by the KK relations to facilitate accurate phase retrieval. In this illumination scheme, the transverse wavevector of the incident plane wave $\mathbf{k}_{inc}$ is the cut-off spatial angular frequency of the pupil function. The complex amplitude of the scattered field, U is expressed in terms of the intensity:

$$U(\mathbf{r}) = \exp\left\{\frac{1}{2}\log\left[I_n(\mathbf{r})\right] - iH\left[\frac{1}{2}\log\left[I_n(\mathbf{r})\right]\right] + i\mathbf{k}_{inc}\cdot\mathbf{r}\right\}, \quad (1)$$

where $\mathbf{r} = x\hat{\mathbf{x}} + y\hat{\mathbf{y}}$, I_n is the captured intensity image corresponding to the nth illumination angle, and $H\{\cdot\}$ denotes the directional Hilbert transform. However, this process requires sequential acquisition of n intensity images with different illumination angles. To enable the single-shot acquisition, we use triangle oblique illuminations to merge three images into one color image based on color-coded illuminations. Three LEDs with respective R/G/B channels are distributed according to the matched illumination condition, as shown in Fig. 1(b). The color image can be acquired in a single exposure and decomposed into three (R, G, and B) channel images [Fig. 1(c)] (see Section A in Supplement 1). Based on the KK relations, we reconstruct the complex amplitude of the object using the three-channel images and take it as the initial value [Fig. 1(d)]. With iterations by the previously proposed iKK-QPI method [18], the intensity images are used to update the real part of the complex amplitude, and the true amplitude and phase of the object can finally be reconstructed [Fig. 1(e)] (see Section C in Supplement 1).

For large-phase objects, the phase at a given wavelength may exceed 2π, making phase unwrapping necessary for accurate quantitative phase retrieval. CMKK-QPI incorporates phase unwrapping into the iterative process, enabling accurate reconstruction of large-phase objects. When color-multiplexed imaging is used, the phase retrieved from different spectral channels must be normalized to a common reference wavelength. Here, we assume negligible chromatic dispersion within the visible range, so that for weakly absorbing samples, the amplitude distribution is nearly identical across the red, green, and blue channels. Under this assumption, each channel is first unwrapped independently and then normalized to the common reference wavelength. In the KK initialization, the resulting phase estimates are combined into the initial estimate. During each subsequent iteration, the phase estimate of each channel is treated in the same way before the synthetic-aperture update. Although the unwrapped phase in the early iterations may still contain errors, these errors gradually decrease rather than diverge during iterative optimization. Details of the phase-unwrapping procedure, wavelength normalization, and reconstruction pseudocode are provided in Section B in Supplement 1.

Three experiments were conducted to validate the effectiveness and practicality of CMKK-QPI. To evaluate the reconstruction accuracy of CMKK-QPI, we initially performed an experiment on a phase resolution target, and the comparative results are shown in Fig. 2. Conventional multi-frame FPM [Fig. 2(a)] was used as a high-quality multi-measurement reference for comparison, whereas the KK relations-based method [Fig. 2(b)]

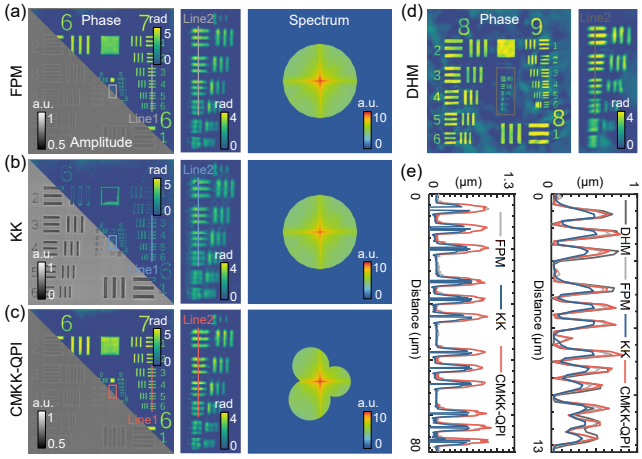

Fig. 2. Comparative results for a phase resolution target. (a)–(c) Amplitude, phase, and spectrum reconstructed by FPM, the KK relations-based method, and CMKK-QPI, respectively. (d) DHM phase reconstruction. (e) Phase profiles along Line 1 and Line 2.

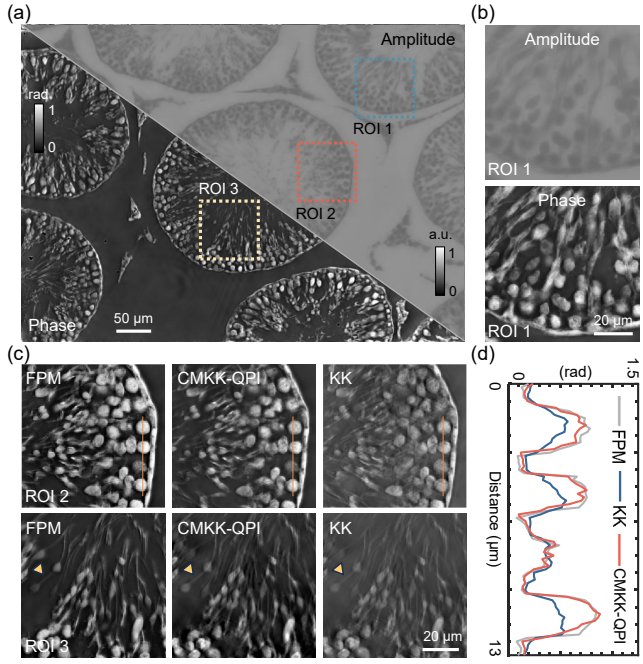

Fig. 3. Comparative experiments on a mammalian vas deferens section. (a) Full FoV amplitude and phase reconstructed by CMKK-QPI. (b) Magnified amplitude and phase distributions views of ROI 1. (c) Phase reconstructions of ROI 2 and ROI 3 by FPM, the KK-based method, and CMKK-QPI. (d) Quantitative phase profiles along the orange lines in (c).

shows clear limitations in reconstructing large phase variations, leading to pronounced phase-unwrapping artifacts and degraded amplitude recovery. In contrast, CMKK-QPI [Fig. 2(c)] yields reconstructions that are visually consistent with the FPM reference while effectively suppressing the unwrapping artifacts observed in the KK-based result. The phase profile along Line 1 [Fig. 2(e)] further shows that CMKK-QPI mitigates the discontinuities in the KK-based reconstruction and retrieves a smoother phase distribution that more closely follows the FPM reference. Although CMKK-QPI uses fewer illumination angles and therefore has a smaller spectrum support than FPM, it still preserves the essential high-frequency information required for high-resolution imaging. In addition, CMKK-QPI converged in only 5 iterations, compared with 15 iterations for FPM (20 raw images), indicating substantially improved computational efficiency. To provide an independent assessment of phase accuracy, we further performed a digital holographic microscopy (DHM) measurement at 532 nm using a 20×, 0.8 NA objective [Fig. 2(d)]. Because the field of view (FoV) of the DHM measurement differs from that of the CMKK-QPI and FPM reconstructions, only the phase profile along Line 2 could be directly compared with DHM [Fig. 2(e)], where the CMKK-QPI result shows the closest agreement and recovers a slightly larger phase range than FPM. CMKK-QPI resolves features down to Group 10, Element 4 (345 nm), close to the theoretical resolution of 328 nm at the central wavelength of 525 nm. These results demonstrate that CMKK-QPI effectively suppresses the unwrapping artifacts of the KK-based method while maintaining high spatial resolution, reliable quantitative phase reconstruction for large-phase objects, and improved computational efficiency.

We subsequently imaged a section of a mammalian vas deferens, and the reconstruction results are shown in Fig. 3. As shown in Fig. 3(a), CMKK-QPI reconstructs both amplitude and phase across the full FoV, clearly revealing the complex cross-sectional structure of the tissue. Figure 3(b) presents magnified views of ROI 1 [blue box in (a)], demonstrating the simultaneous recovery of fine high-contrast absorption features and optical thickness variations, which cannot be obtained from a conventional single-frame intensity measurement. For reconstruction fidelity assessment, Fig. 3(c) compares the phase results for ROI 2 (red box) and ROI 3 (yellow box) reconstructed by FPM, the KK relations-based method, and CMKK-QPI. The KK relations-based method fails to accurately recover the large phase variations inherent in the tissue, leading to phase underestimation. In contrast, CMKK-QPI shows high consistency with FPM and accurately delineates the distribution of spermatozoa within the lumen. This is further confirmed by the profiles in Fig. 3(d), where the CMKK-QPI curves closely follow the FPM profiles, whereas the KK-based method shows substantial deviation at large phase values. Although the finest high-frequency details in the CMKK-QPI reconstruction are slightly inferior to those in the FPM result, which required 12 raw images and 15 iterations, CMKK-QPI achieved this performance using only a single color image and 5 iterations. These results demonstrate that CMKK-QPI improves imaging efficiency and temporal resolution while maintaining high reconstruction quality, highlighting its potential for dynamic biological imaging.

Finally, we conducted experiments on two types of live cell samples to validate the capability of CMKK-QPI for dynamic biological imaging. The comparative results for PLC cells are presented in Fig. 4(a). The magnified views in Fig. 4(b) clearly visualize fine subcellular structures, such as the nucleus, nucleolus, and lipid droplets, as reconstructed by the three methods, while Fig. 4(c) provides line profiles for quantitative comparison. Consistent with previous experimental conclusions, CMKK-QPI achieves high-fidelity phase reconstruction. As illustrated in Fig. 4(d), the computation time of CMKK-QPI is comparable to that of the KK relations-based method, yet it attains reconstruction precision and quality on par with the multi-frame FPM technique. This indicates that CMKK-

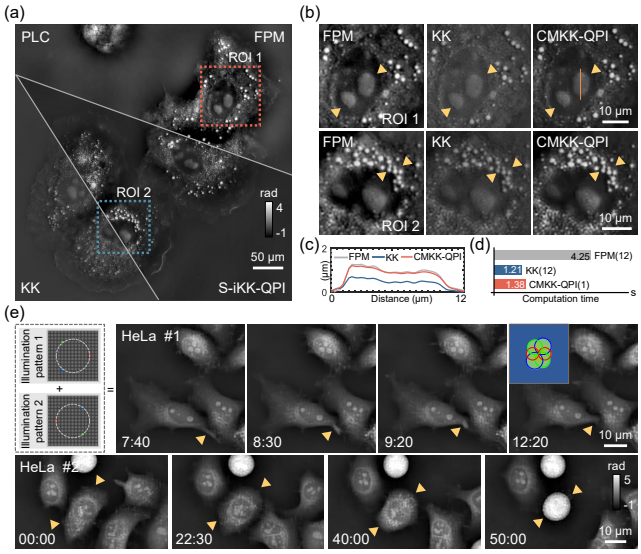

Fig. 4. Comparative experiments on live cell samples. (a) Phase of PLC cells reconstructed by FPM, the KK-based method, and CMKK-QPI. (b) Magnified views of the red and blue boxed regions in (a). (c) Line profiles along the orange line in (b). (d) Computation time for the reconstructions in (a). (e) Color-multiplexed illumination patterns and CMKK-QPI phase of dynamic morphological changes in HeLa cells.

QPI significantly enhances imaging efficiency while drastically reducing data throughput.

We also conducted a 50-minute continuous observation of dynamic morphological changes in live HeLa cells (see Visualization 1). Under a static tri-color illumination pattern, each frame samples three sub-apertures, so the accessible Fourier-space coverage is not perfectly uniform [see Fig. 1(e)]. Although this configuration already enables reliable reconstruction, a more uniform spectral distribution can further improve reconstruction completeness and stability. In dynamic imaging, the temporal continuity between adjacent frames allows improved Fourier-space coverage across time without increasing the number of exposures required for each reconstructed frame and thus without reducing the imaging frame rate (see Section D in Supplement 1 for detailed analysis). To this end, we adopted an alternating illumination strategy during acquisition. As illustrated in Fig. 4(e), a second illumination mode (illumination pattern 2) was generated by rotating the three RGB LEDs along the annular illumination. Combined with a sliding-window reconstruction strategy, spectral information from the preceding frame was jointly used to assist reconstruction of the current frame, effectively achieving six-sub-aperture coverage in the Fourier domain and yielding improved reconstruction quality and stability for dynamic monitoring [Fig. 4(e)]. As shown in the first row, CMKK-QPI captured rapid morphological fluctuations of the cell within 1 minute and 40 seconds. The observed filopodia retraction further demonstrates its capability for high-speed imaging while preserving fine spatial details. The second row shows a morphological transformation characteristic of a cell preparing for mitosis. During this process, the cell changes from a spread state to a spherical shape, accompanied by a substantial increase in optical path length. Despite this large phase variation, CMKK-QPI maintains accurate quantitative phase retrieval without unwrapping artifacts. These results demonstrate that CMKK-QPI enables robust long-term, high-resolution live-cell monitoring with minimal data redundancy.

In summary, we have demonstrated CMKK-QPI, a color-multiplexed single-shot QPI framework that integrates spectral encoding with iterative KK-based retrieval for high-speed, high-precision imaging. By encoding angular information into spectral channels, CMKK-QPI enables single-shot acquisition, while KK-based initialization followed by iterative refinement overcomes the limitation of conventional single-shot techniques to pure-phase objects. This design enables the simultaneous reconstruction of both amplitude for weakly absorbing specimens and phase for large phase delays, capabilities that are often inaccessible to standard methods. With only 5 refinement iterations, CMKK-QPI achieves reconstruction quality comparable to multi-frame FPM while reducing data redundancy to a single exposure and enabling real-time QPI at 30 Hz. In this way, CMKK-QPI effectively balances temporal resolution, phase accuracy, and computational efficiency. The combination of single-shot acquisition, KK-based initialization, and minimal iterative refinement enables CMKK-QPI to bridge the gap between imaging speed and reconstruction fidelity in non-interferometric QPI. The successful visualization of rapid subcellular dynamics, including filopodia extension and cell rounding, further demonstrates its robustness for dynamic biological imaging. With its simple hardware configuration and strong performance, CMKK-QPI offers a promising tool for high-throughput, label-free live-cell microscopy.

Funding. National Key Laboratory of Plasma Physics (JCKYS2024212804); National Key Research and Development Program of China (2022YFA1205002, 2024YFE0101300, 2024YFF0505603, 2024YFF0505600); National Natural Science Foundation of China (62227818, 62361136588, 62305162, U21B2033, 62505136, 62575139).

Disclosures. The authors declare no conflicts of interest.

Data availability. No data were generated or analyzed in the present research.

Supplemental document. See Supplement 1 for supporting content

REFERENCES

1. T. Kim, R. Zhou, L. L. Goddard, *et al.*, Laser Photon. Rev. **10**, 13 (2016).
2. Y. Park, C. Depeursinge, and G. Popescu, Nat. Photon. **12**, 578 (2018).
3. R. Cao, C. Shen, and C. Yang, Nat. Commun. **15**, 4713 (2024).
4. P. C. Chaumet, P. Bon, G. Maire, *et al.*, Light. Sci. Appl. **13**, 288 (2024).
5. P. Gao and C. Yuan, Light. Adv. Manuf. **3**, 105 (2022).
6. Z. Huang and L. Cao, Light. Sci. Appl. **13**, 145 (2024).
7. S. B. Mehta and C. J. Sheppard, Opt. Lett. **34**, 1924 (2009).
8. L. Tian and L. Waller, Opt. Exp. **31**, 11804 (2023).
9. M. R. Teague, J. Opt. Soc. Am. **73**, 1434 (1983).
10. C. Zuo, J. Li, J. Sun, *et al.*, Opt. Lasers Eng. **135**, 106187 (2020).
11. G. Zheng, R. Horstmeyer, and C. Yang, Nat. Photon. **7**, 739 (2013).
12. X. Ou, G. Zheng, and C. Yang, Opt. Express **22**, 4960 (2014).
13. C. Zuo, J. Sun, and Q. Chen, Opt. Express **24**, 20724 (2016).
14. J. Sun, Q. Chen, J. Zhang, *et al.*, Opt. Lett. **43**, 3365 (2018).
15. C. Lee, Y. Baek, H. Hugonnet, *et al.*, Opt. Lett. **47**, 1025 (2022).
16. X. Chen, S. Yao, J. Song, *et al.*, Opt. Lett. **49**, 3512 (2024).
17. J. M. Cowley, *Diffraction Physics* (Elsevier, 1995).
18. Q. Shen, J. Sun, S. Zhou, *et al.*, Opt. Lett. **50**, 1144 (2025).
19. Y. Baek and Y. Park, Nat. Photon. **15**, 354 (2021).
20. S. Li, B. Wang, H. Guan, *et al.*, Opt. Lett. **50**, 1457 (2025).
21. J. Sun, C. Zuo, J. Zhang, *et al.*, Sci. Rep. **8**, 7669 (2018).
22. Y. Wu, Y. Zhang, W. Luo, *et al.*, Sci. Rep. **6**, 28601 (2016).
23. S. Zhou, J. Li, J. Sun, *et al.*, Optica **9**, 1362 (2022).
24. S. Zhou, Q. Shen, H. Ullah, *et al.*, Adv. Photon. **8**, 026003 (2026).